Supporting Information

Optimizing perovskite solar cell architecture in multi-step routes including electrodeposition

Mirella Al Katrib [1], Lara Perrin [1,*], and Emilie Planes [1]

[1] Univ. Grenoble Alpes, Univ. Savoie Mont Blanc, CNRS, Grenoble INP, LEPMI, 38000 Grenoble, France
*Email: Lara.Perrin@univ-smb.fr

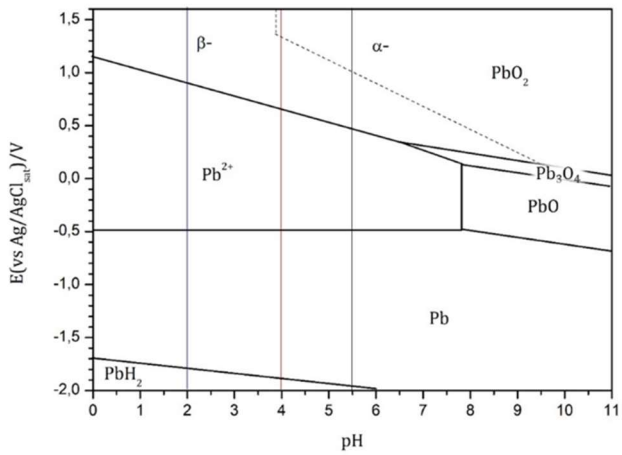

Figure S1: Pourbaix diagram of lead (potential values were adapted from Hyde et al. values, according to the potential of our reference electrode)

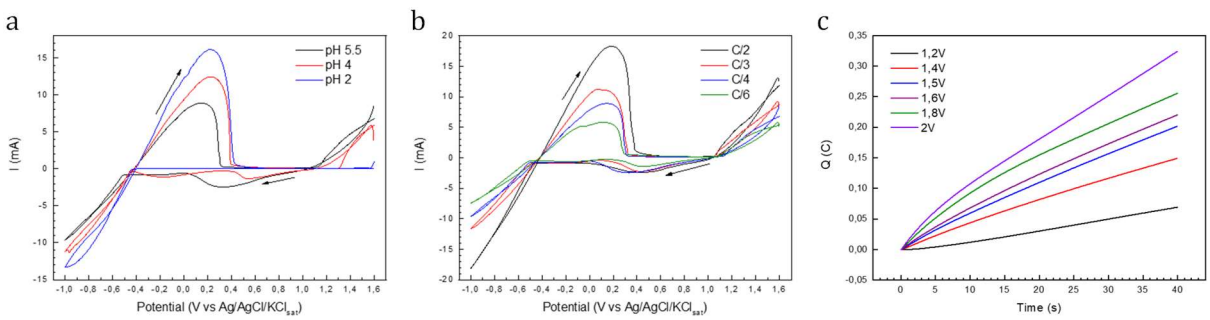

Figure S2: Cyclic voltammograms of the aqueous solution of $Pb(CH_3COO)_2{\cdot}3H_2O$ and $NaNO_3$ (1:2) obtained (a) at different pH values for the concentration C/4 (scan rate = 50mV/s), (b) with different electrolyte concentrations having a pH of 5.5 (scan rate = 50 mV/s) ; (c) Chronocoulometry curves showing the variation of the charge as a function of time during electrodeposition of PbO_2 at different potential values for the concentration C/4 and a pH of 5.5 (example curves for ITO substrate)

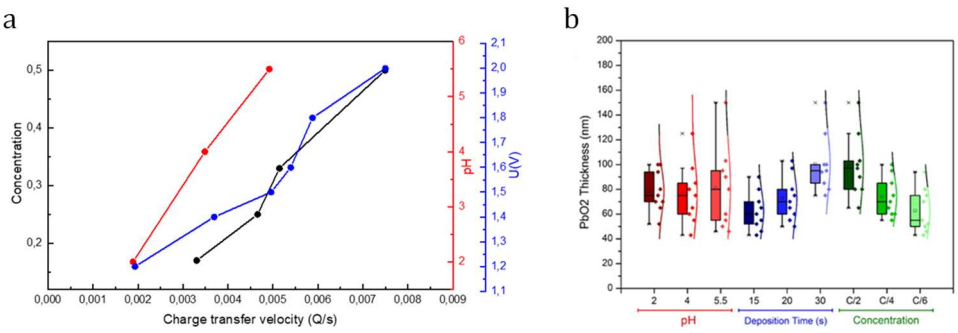

Figure S3: a) Impact of the concentration of the electrolyte, the pH of the electrolyte and the applied potential on the slope variation of chronocoulometry curves (for pH data, the concentration was fixed at C/4 and the potential at 1.5 V; for concentration data, the pH was fixed at 5.5 and the potential at 1.5 V); (b) Boxplot showing the variation of PbO_2 thickness deposited on ITO for different pH values, different deposition times and different electrolyte concentrations (only the potential was fixed at 1.5V)

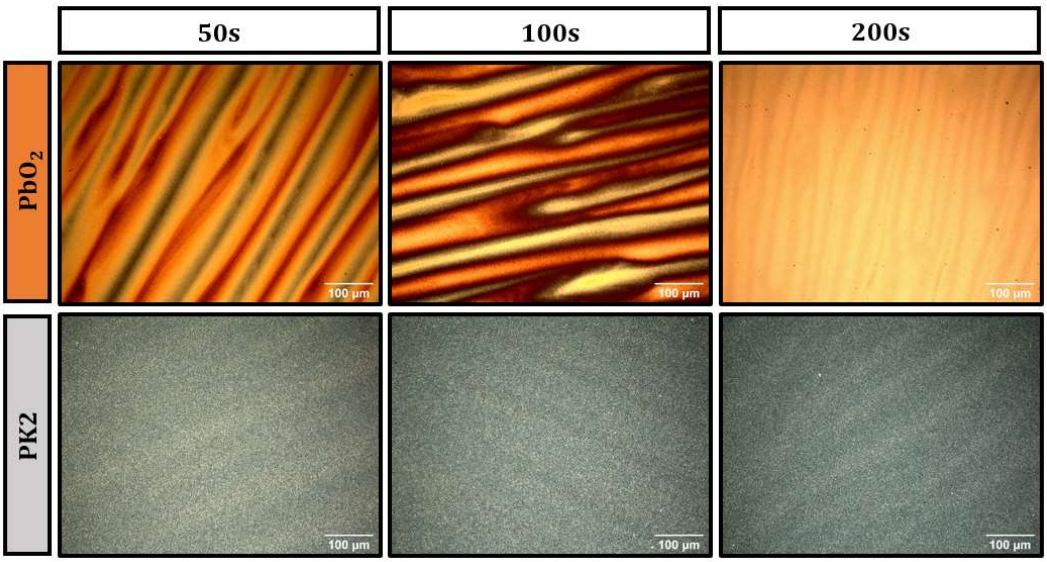

Figure S4: Optical Microscopy images of PbO_2 electrodeposited on mesoporous TiO_2 for 50s, 100s and 200s, and when converted to PK2

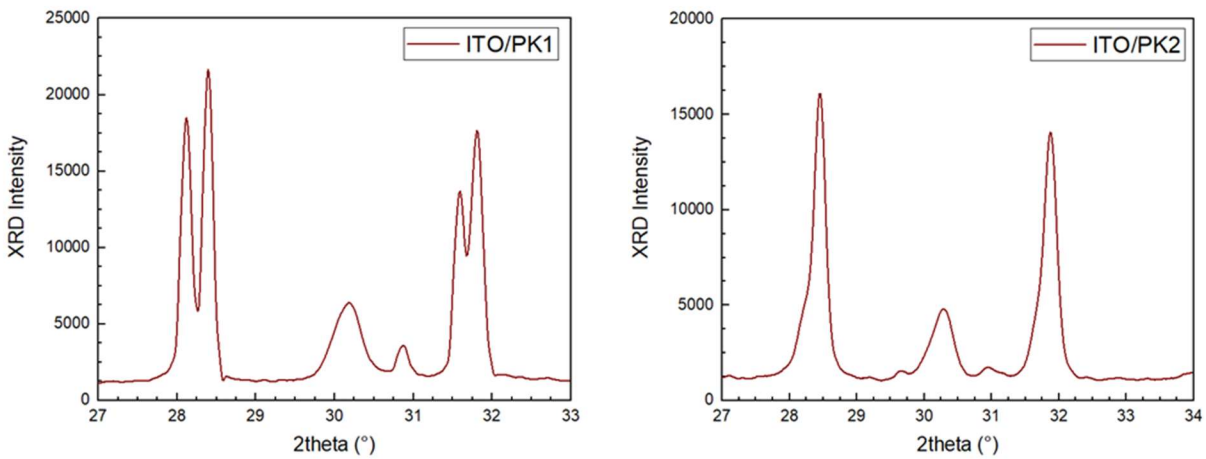

Figure S5: Enlarged XRD patterns of PK1 and PK2 deposited on ITO, showing the (004)-(220) and (114)-(222) double peaks

Table S1: Ratio of (001) PbI_2 phase and (004) $MAPbI_3$ phase with respect to (002) $MAPbI_3$ phase, calculated using XRD patterns of PK1 and PK2 on three different substrates

	PbI_2 (001) / $MAPbI_3$ (002) %	**$MAPbI_3$ (004)/(002) %**
ITO-PK1	1.84	87.35
ITO-PK2	32.78	84.57
SnO_2-PK1	45.24	105.98
SnO_2-PK2	30.75	77.82
TiO_2-PK1	4.30	78.73
TiO_2-PK2	4.24	81.95

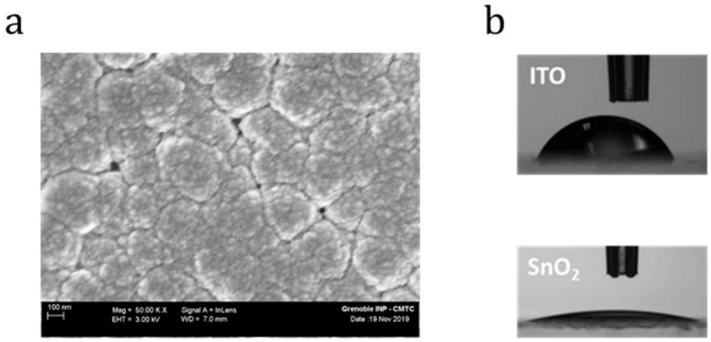

Figure S6: a) Top-view SEM images of PbO_2 deposited on SnO_2 with higher magnitude ; b) Typical optical images of water contact angle measurements by the sessile drop method for both ITO and SnO_2 substrates

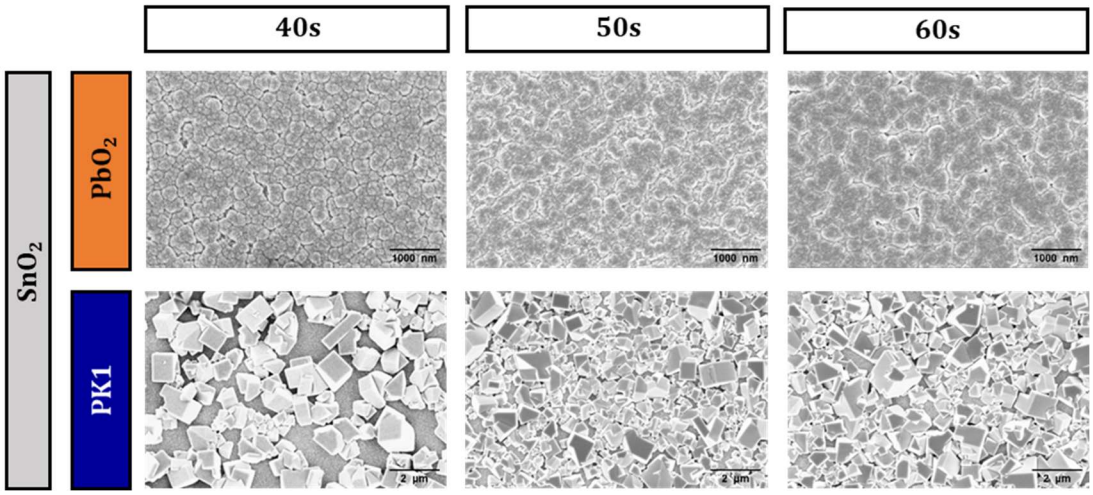

Figure S7: Top-view SEM images of SnO_2/PbO_2 and SnO_2/PK1 for electrodeposition duration of respectively 40, 50 and 60s.

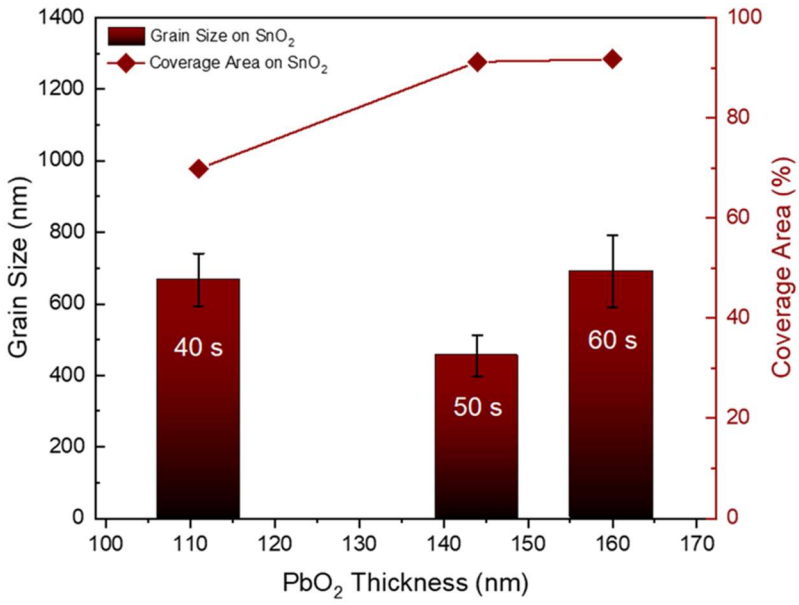

Figure S8: The variation of coverage area and grain size for PK1 perovskite with respect to PbO_2 layer thickness (values indicated in seconds are for the corresponding PbO_2 deposition time)

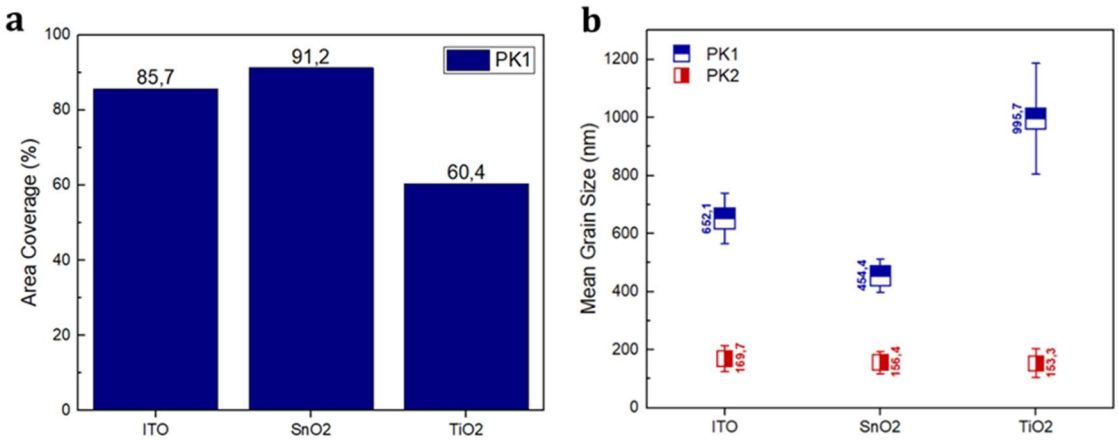

Figure S9: Variation of a) the area coverage of PK1 on ITO, SnO_2 and m-TiO_2 and b) the grain size of PK1 and PK2 on the three substrates (for a PbO_2 electrodeposition duration of 50s)

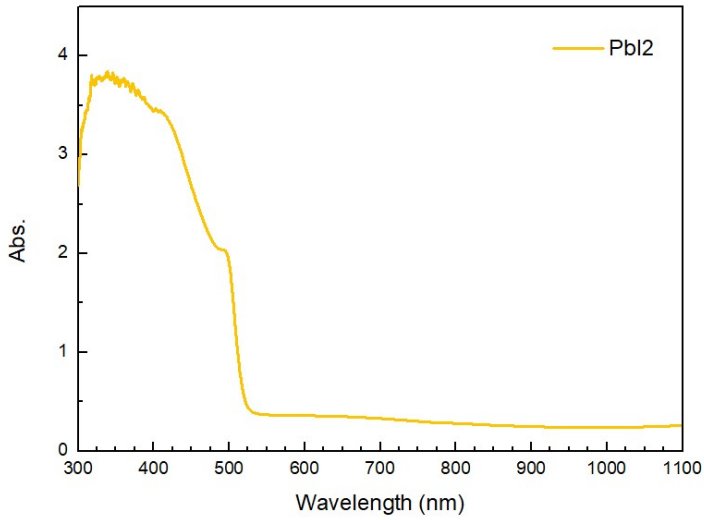

Figure S10: UV-visible absorption spectrum of PbI_2 converted from PbO_2 on ITO

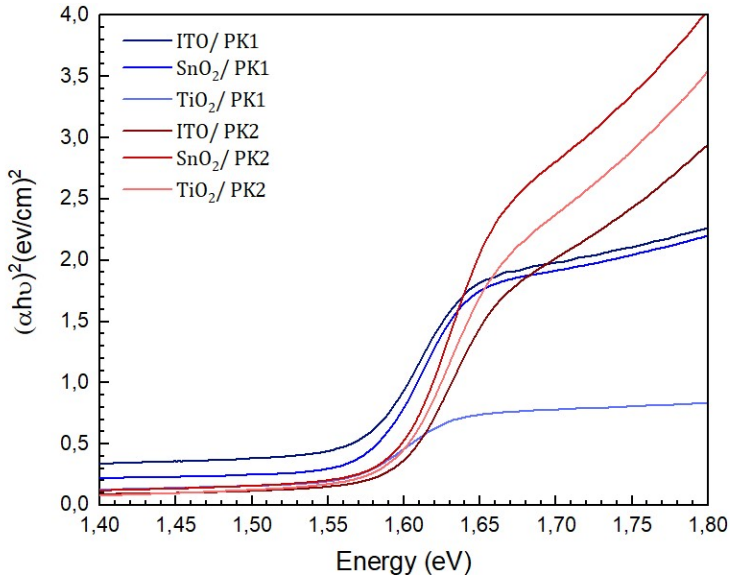

Figure S11: Tauc plots of PK1 and PK2 on ITO, SnO_2 and m-TiO_2 drawn using UV-visible absorption data

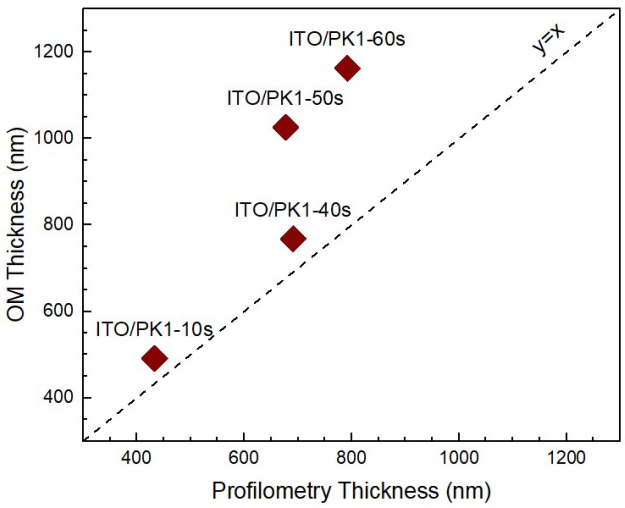

Figure S12: Thickness calculated using optical microscopy for PK1 deposited on ITO for 4 different durations, with respect to their thickness measured using profilometry

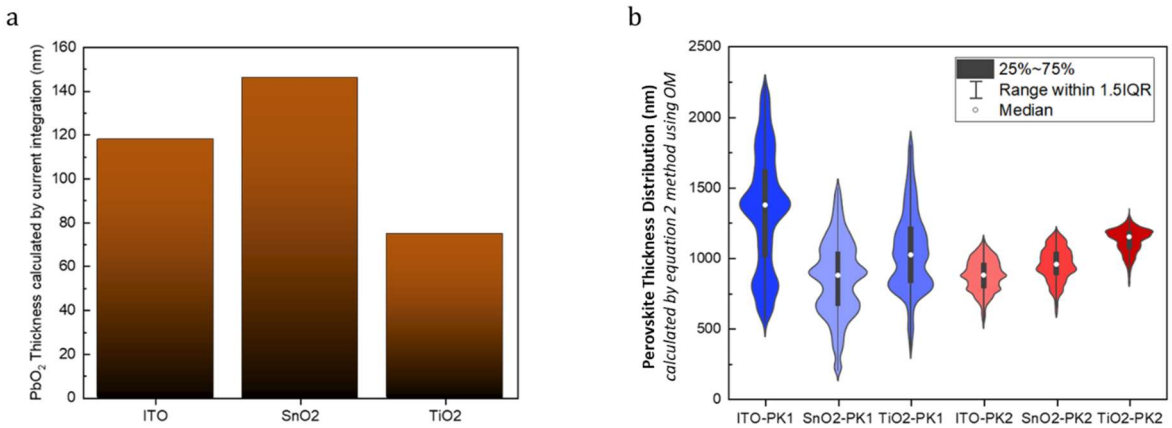

Figure S13: a) Thicknesses of PbO_2 layers used for PK1 and PK2 perovskite conversions presented in Figure S13-b ; b) Violin Plot representing the thickness distribution of PK1 and PK2 obtained on ITO, SnO_2 and m-TiO_2 substrates

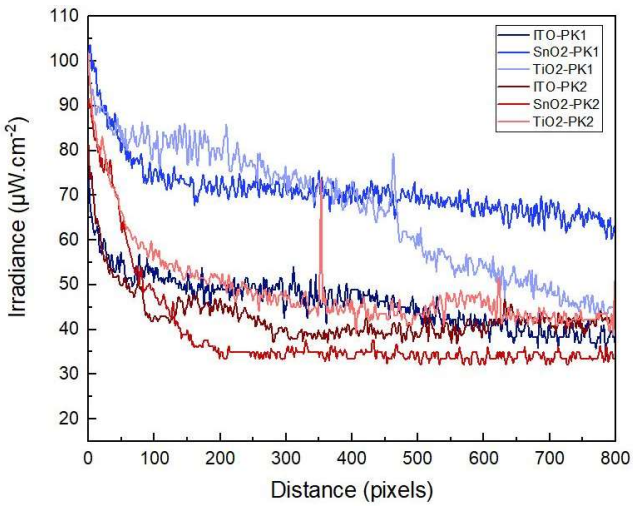

Figure S14: Profile plot showing the variation of the PL Scale of Figure 5c along a vertical line in the center of the PK1 and PK2 films, going from the top to the bottom

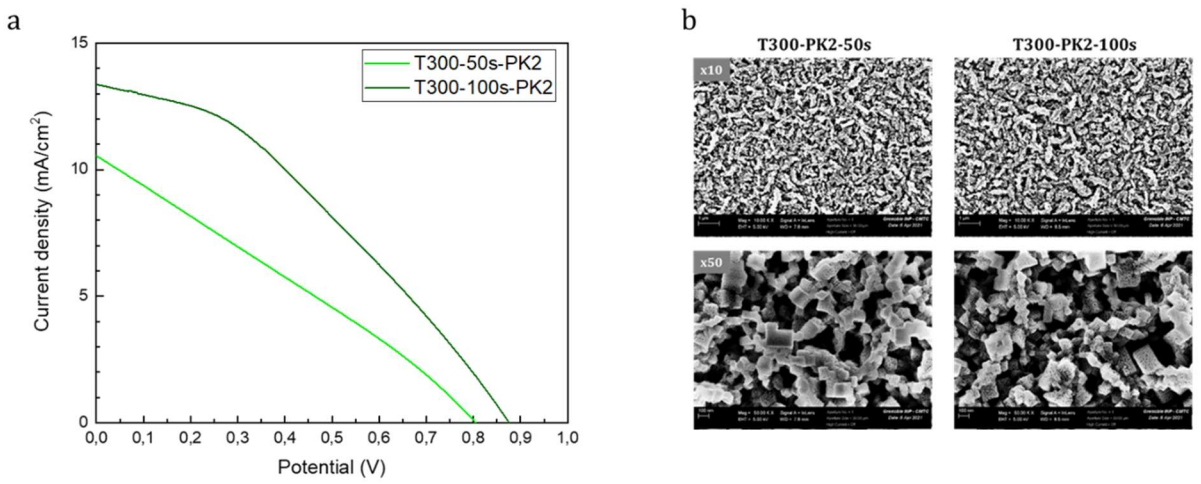

Figure S15: a) J(V) curves on m-TiO_2 (300nm thickness) for two PK2 layers obtained according to PbO_2 initiator deposition durations of 50s et 100s (Glass/ITO/c-TiO_2/m-TiO_2/$MAPbI_3$ (PK2)/P3HT/C architecture, 0.1 cm^2) ; b) Top-view SEM images for these two PK2 layers

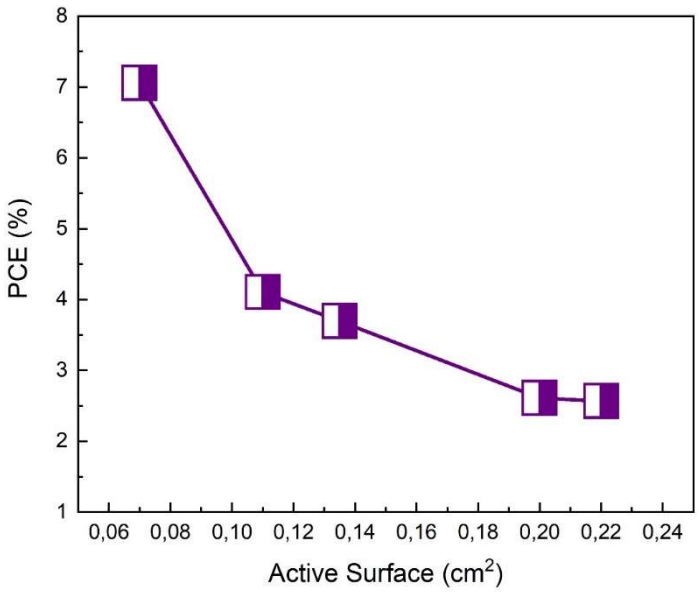

Figure S16: Scatter plot showing the variation of the PCE with respect to the active surface of the solar cells Glass/ITO/c-TiO_2/m-TiO_2/$MAPbI_3$ (PK2)/P3HT/C

Experimental: Optimization of conversion parameters for PK1

To optimize the conversion parameters of PbO_2 into PK1, PbO_2 samples electrodeposited on ITO for 15s were immersed in a 16 mg/mL MAI solution, and the conversion was observed at 40°C while changing the duration, or while fixing the duration for 3 min and variating the conversion temperature. The observations are noted in Tables S2 and S3.

Table S2: Observed results of PK1 conversion for a fixed temperature of 40°C and different conversion durations.

T °C	Duration	Results
40 °C	3 min	Color change observed
40 °C	10 min	Color change observed
40 °C	30 min	Partial degradation
40 °C	60 min	Nearly total degradation

Table S3: Observed results of PK1 conversion for a 3 min duration and different temperatures.

T °C	Duration	Results
30 °C	3 min	Color change observed
40 °C	3 min	Color change observed
50 °C	3 min	Partial degradation

Figure S17 shows the variation of PK1 thickness when changing the PK conversion parameters (for PbO_2 samples electrodeposited for 15s). The XRD patterns in Figure S18 indicates that the PbI_2 ratio in the sample increases when increasing the temperature and the conversion duration. The best relative crystallinity for perovskite was for a conversion at 40°C for 3 min (Table S4).

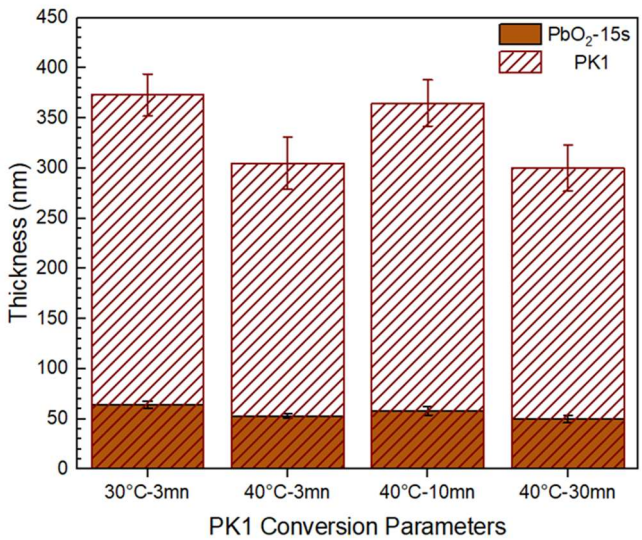

Figure S17: PK1 thickness variation for different PK conversion parameters (thickness of used initial PbO_2 samples is indicated for exact comparison).

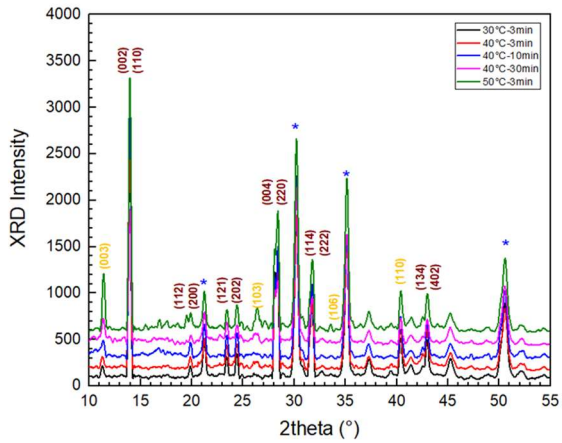

Figure S18: XRD patterns of PK1 converted at different temperatures and durations

Table S4: Relative crystallinity (χ) of PK1 for different conversion parameters

	χ %
3 min- 40°C	9.8
10 min- 40°C	6.2
30 min- 40°C	4.85
3 min- 50°C	9.5
3 min- 30°C	9.7

Before to select a perovskite conversion bath concentration corresponding to 16mg/mL of MAI (0.1M), the effect of the MAI concentration was studied. Figure S19 illustrates the case of a conversion fixed at 40°C for 3 min. Increasing the concentration will increase the band gap and the absorbance of the perovskite. A blue shift in the PL spectra of PK1 is also observed when increasing the MAI concentration, which may indicate a change in the morphology, thickness or grain size.

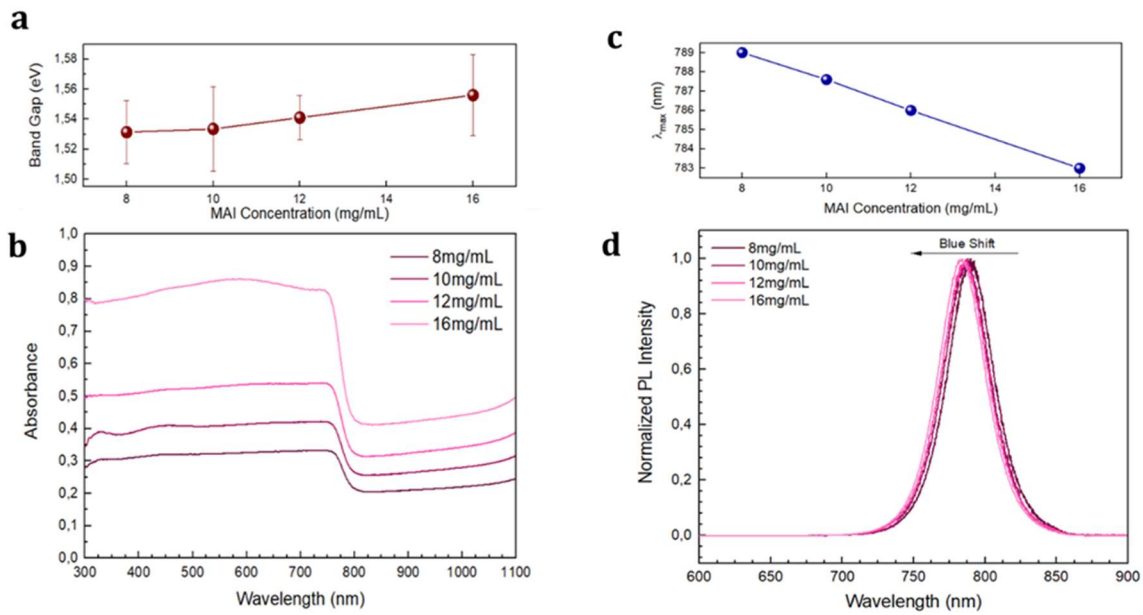

Figure S19: a) Band Gap, b) UV-visible absorption spectra, c) λmax of emission and d) Photoluminescence spectra of PK1 when variating the MAI concentration between 8 mg/mL and 16 mg/mL